Linearization of the Fifth Generation Power Amplifiers by Injection of the Second Order Digitally Processed Signals

Aleksandar ATANASKOVIC [1], Aleksandra DJORIC [1], Natasa MALES ILIC [1], Biljana P. STOSIC [1], Djuradj BUDIMIR [2]

[1] Dept. of Telecommunication, University of Nis, Aleksandra Medvedeva 14, 18000 Nis, Serbia
[2] Wireless Communications Research Group, School of Computer Science and Eng., University of Westminster, 115 New Cavendish Street, W1W 6UW, London, UK

{aleksandar.atanaskovic, natasa.males.ilic, aleksandra.djoric, biljana.stosic}@elfak.ni.ac.rs, d.budimir@wmin.ac.uk

Submitted January 9, 2024 / Accepted April 2, 2024 / Online first May 28, 2024

Abstract. *This paper conducts a validation of two linearization approaches that utilize baseband nonlinear linearization signals of the 2nd order, through practical experiments on an asymmetrical two-way microstrip Doherty amplifier (ADA), and simulations on a symmetrical two-way Doherty amplifier (DA) as well as the single stage power amplifier (PA) for the post-OFDM 5G modulation formats. In the first approach, linearization signals are led at the input and output of the carrier transistor in the DA, while in the second approach, they are injected at the outputs of both the carrier and peaking amplifiers. The DA was tested in simulation for the FBMC signal of 20 MHz bandwidth, while the experimental measurements were performed for the FBMC signal on the ADA for different useful signal frequency bandwidths, 5 MHz, 7.5 MHz, and 10 MHz. The maximal improvement of DA linearity obtained in simulation is 10 dB for lower power and 5 dB for maximum amplifier output power, while the second approach gives around 2 dB better results for higher power levels. The experimental test for ADA performed for considered signal bandwidths indicates 3 dB to 5 dB linearity improvement for the implemented approaches and more symmetrical results achieved by the second approach. Additionally, the simulation tests for the PA were carried out for the FBMC, UFMC, and FOFDM signals of 100 MHz bandwidth, with the application of the first linearization approach. The minimal achieved linearization improvement is 13 dB for the FOFDM signal and a maximal of 18 dB for the FBMC signal.*

Keywords

The post-OFDM 5G modulations, broadband power amplifier, Doherty amplifier, baseband signal, second harmonic, linearization

1. Introduction

The Fifth Generation network standard (5G) characterized by increased data speeds, low latency, a massive connection of devices, reliability, increased battery life, and very high bandwidth is of great challenge for the 5G wireless system design [1], [2]. The promising 5G frequency band below 6 GHz is at 3.5 GHz (3.4–3.8 GHz) which enables satisfactory coverage despite the limitation due to band congestion. Band above 6 GHz at the mm-wave bands, e.g. at the 26 GHz (24.25–27.5 GHz), offers spectrum availability with high bandwidth that provides increased data rates and low latency, but high free space attenuation leads to coverage restriction. Wider areas coverage can be enabled in lower frequency bands of interest such as 0.7 GHz, 0.95 GHz and 1.5 GHz. Therefore, this combination of low, mid and high frequency bands is suggested for the fulfilment of the 5G network requirements. With the aim to improve the energy efficiency and linearity of the 5G system new waveforms are suggested that achieve better spectral efficiency for different scenarios. Leading candidates of the modulation formats to overcome limitations and provide adequate 5G system quality are: Filter Bank Multi-Carrier (FBMC), Universal Filtered Multi-Carrier (UFMC), and Filtered Orthogonal Frequency Division Multiplexing (FOFDM).

A variety of techniques for amplifier linearization such as feedforward, feedback, predistortion [3] and different approaches of digital predistortion [3], [4] can be found in the literature. The authors of this paper anteriorly developed the digital linearization approach (DEB_LIN) [5–8] that uses the 2nd order digital signals adequately processed in magnitude and phase angles in the baseband, which then modulate the 2nd harmonic of the fundamental carrier. The generated linearization signals are injected at the gate and drain (input and output) of the PA transistor. The results of

DOI: 10.13164/re.2024.0339

the linearization obtained by this linearization approach in the simulation were already published for the single stage PA [5], [6] and the two-way DA [8], and tested for QAM, WCDMA, OFDM and LTE modulation schemes. Also, the linearization results were published for the single stage PA that operates in frequency around 3.5 GHz for UFMC, FBMC, and FOFDM modulation schemes with 50 MHz useful signal bandwidth [7]. The DEB_LIN approach was validated in experiments using the asymmetrical two-way microstrip Doherty amplifier for both the 16QAM signal with a 1 MHz frequency bandwidth and the 64QAM signal with a 2 MHz frequency bandwidth [6], [8]. The linearization of the DA in simulation and the ADA in experiments was performed in [8] by injecting the formed signals for the linearization at the input and output of the carrier amplifier stage (approach-1), or at the outputs of both carrier and peaking amplifiers (approach-2) at the Doherty amplifier configuration.

To extend our research, in this paper, we tested, in simulation and experiments, the single stage PA and Doherty amplifiers in symmetrical and asymmetrical configuration for 5G modulation formats of wider frequency bandwidths than in previously presented results. We analyzed the behavior:

a) in the simulation of the single stage PA when source signals are post-OFDM 5G signals FBMC, UFMC, and FOFDM at carrier frequency 3.5 GHz with 100 MHz bandwidth;

b) in the simulation of the symmetrical DA when the digital linearization approaches (approach-1 and approach-2) were applied for the FBMC modulation at carrier frequency 0.95 GHz with 20 MHz bandwidth in the range of the useful signal power;

c) in the experiment of approach-1 and approach-2, applied on the fabricated asymmetrical DA for the 5G FBMC signal at carrier frequency 0.9 GHz for different useful signal frequency bandwidths (5 MHz, 7.5 MHz, and 10 MHz).

Compared to the results attained in our previous research [5–8] it can be observed that the linearization achieved in simulation for QAM, OFDM, LTE and FBMC signals of the same bandwidth is of similar order depending on useful signal power level, i.e. when the power increases, the linearization effect of the applied technique deteriorates. Additionally, as it can be expected, experimental results indicate better linearization improvement for less signal bandwidths of 1 MHz and 2 MHz achieved earlier in [6], [8] by around 2 dB than for wider (5 MHz, 7.5 MHz, and 10 MHz) bandwidths considered in this paper and the same behavior of the approach-1 and approach-2 as in previous results, that is a small improvement by applying 2nd approach.

The paper is organized in the following manner: After the introduction, Section 2 is devoted to the 5G modulation schemes; Section 3 explains the theory that describes the behavior of the applied DEB_LIN approaches; Sections 4 and 5 include description and characterization of the single stage PA and symmetrical DA with the linearization circuit, respectively, and the illustration of the simulated linearization results; Section 6 describes the measurement setup; Section 7 represents linearization results gained through experimental measurements for the asymmetrical DA; conclusion and list of used literature are given at the end of the paper.

2. The 5G Modulation Formats

Filter Bank Multi-Carrier modulation uses filtering of each sub-carrier individually rather than the whole subband to transmit data. Respecting the Nyquist rate, the post-OFDM signal such as FBMC can accomplish better spectral efficiency and flexibility to imperfect synchronization compared to CP-OFDM since it does not use the cyclic prefix (CP) [9], [10]. FBMC has low side lobe levels and a steep slope at the edges of the signal band as it is controlled in the frequency and time domain by using prototype filters that provide spectrum confinement and orthogonality among adjacent sub-carriers. Moreover, FBMC uses a larger number of subcarriers in contrast to CP-OFDM, which leads to more spectral efficiency at the output of the wireless transmitter. FBMC is a vital post-OFDM candidate for the 5G wireless transmitters whose features are kept acceptable over a wide bandwidth since this modulation scheme possesses lower out-of-band emissions in comparison with CP-OFDM. The low complexity of FBMC signal processing is an essential advantage over the other post-OFDM 5G modulation candidates.

Universal Filtered Multi-Carrier (UFMC) as another post-OFDM 5G signal possesses some characteristics of CP-OFDM, such as high PAPR (peak to average power ratio), flexibility and MIMO properties, but also overcomes the disadvantages of CP-OFDM. UFMC provides a shorter impulse response in the time domain by filtering a group of consecutive sub-carriers. As a consequence, out-of-band emissions and inter-symbol interference between the adjacent channels are reduced [9]. UFMC has smaller guard bands in adjacent channels which make it more spectrally efficient in reference to CP-OFDM. However, UFMC is a complex system due to the block filtering that defines the number of DFT (Discrete Fourier Transform) operations. The energy efficiency, which is very important in a practical system application, is reduced by increasing system complexity tightly influenced by the DFT number.

Filtered Orthogonal Frequency Division Multiplexing even though has a similar transmitter structure as UFMC utilizes a CP, [9]. Additionally, residual inter-symbol interference (ISI) usually appears. However, ISI that has the power at the order of noise can be neglected, since the filter in FOFDM can have better attenuation outside the band than that in UFMC. Also, effective channel coding can additionally prevent performance degradation. The subcarrier spacing and the CP length in FOFDM may be different between the users, which is not the case in UFMC systems. The soft-truncated sinc filter, appropriate for various applications, which is usually used in FOFDM, enables FOFDM to be flexible in the frequency multiplexing.

3. Theoretical Background of the Linearization Approach

A Taylor-series polynomial without memory effect that models a nonlinearity of the amplifier transistor [11] is adequate for the theoretical explanation of the operational mechanism of the used linearization approaches. Amplifier transistors utilized in simulations were modeled by the nonlinear models available in the manufacturers' catalog.

Equation (1) provides the relationship between the FET output current, i_{out}, and the transistor input voltage ($v_{\mathrm{tic/tip}}$) and transistor output voltage ($v_{\mathrm{toc/top}}$), [5, 6, 8]. In this context, $g_{\mathrm{m}x}$ represents the transconductance terms, $g_{\mathrm{d}y}$ denotes the drain-conductance term, while $g_{\mathrm{m}x\mathrm{d}y}$ represents the mixed terms (where the order of each coefficient is determined as $x + y$). The prefixes ic and oc correlate to the input and output of the carrier PA transistor respectively, while the prefixes ip and op relate to the input and output of the peaking PA transistor in the Doherty topology.

$$\begin{aligned} i_{\mathrm{out}} &= g_{\mathrm{m1}} v_{\mathrm{tic/tip}} + g_{\mathrm{m2}}\left(v_{\mathrm{tic/tip}}\right)^2 + g_{\mathrm{m3}}\left(v_{\mathrm{tic/tip}}\right)^3 + \\ &+ g_{\mathrm{d1}} v_{\mathrm{toc/top}} + g_{\mathrm{d2}}\left(v_{\mathrm{toc/top}}\right)^2 + g_{\mathrm{d3}}\left(v_{\mathrm{toc/top}}\right)^3 + \\ &+ g_{\mathrm{m1d1}} v_{\mathrm{tic/tip}} v_{\mathrm{toc/top}} + g_{\mathrm{m2d1}}\left(v_{\mathrm{tic/tip}}\right)^2 v_{\mathrm{toc/top}} + g_{\mathrm{m1d2}} v_{\mathrm{tic/tip}}\left(v_{\mathrm{toc/top}}\right)^2 \end{aligned} \tag{1}$$

The previously performed analysis [5, 6, 8, 11] showed us that some nonlinear terms can be neglected (g_{d1} to g_{d3}) because they have a negligible influence on the intermodulation products, while certain terms create a drain current at the IM3 (the 3rd order intermodulation products) frequencies of opposite phases, so they cancel out each other to a certain degree (g_{m1d2} and g_{m2d1}) and they are excluded from the final equations that relate to the IM3 of the DA output current. However, they are incorporated into the equations that describe the DA output current related to the IM5 products (the 5th order intermodulation products) for an easier explanation of how injected linearization signals influence those nonlinear products.

The baseband signals used for the linearization are created through suitable processing of the in-phase (I) and quadrature-phase (Q) components of the digital signal. This processing results in two components which are the products of the nonlinearity of the 2nd order: the in-phase linearization component, $I_{\mathrm{IM2}} = (I^2 - Q^2)$, and the quadrature-phase linearization component, $Q_{\mathrm{IM2}} = 2IQ$. These components are adequately modified in magnitude by $m_{\mathrm{ic/oc/op}}$ and phase by $\varphi_{\mathrm{ic/oc/op}}$.

In these approaches, the baseband signals, prepared as described, modulate the second harmonic of the fundamental carrier. In the first linearization approach (approach-1), used for the DA linearization, the linearization signals are injected at the input (along with the fundamental signal) as defined by (2), and at the output of the carrier amplifier transistor in the Doherty circuit, as shown in (3). In the second approach (approach-2), the linearization signals are inserted at the transistor output of both the carrier (3) and peaking stages (4) in the DA.

$$\begin{aligned} v_{\mathrm{tic}} &= v_{\mathrm{ic}}\left[I\cos(\omega_0 t) - Q\sin(\omega_0 t)\right] + \\ &+ m_{\mathrm{ic}}\,\mathrm{e}^{-\mathrm{j}\varphi_{\mathrm{ic}}}\,\frac{1}{2}\left[\left(I^2 - Q^2\right)\cos(2\omega_0) - 2IQ\sin(2\omega_0)\right], \end{aligned} \tag{2}$$

$$\begin{aligned} v_{\mathrm{toc}} &= v_{\mathrm{oc}}\left[I\cos(\omega_0 t) - Q\sin(\omega_0 t)\right] + \\ &- m_{\mathrm{oc}}\,\mathrm{e}^{-\mathrm{j}\varphi_{\mathrm{oc}}}\,\frac{1}{2}\left[\left(I^2 - Q^2\right)\cos(2\omega_0) - 2IQ\sin(2\omega_0)\right], \end{aligned} \tag{3}$$

$$\begin{aligned} v_{\mathrm{top}} &= v_{\mathrm{op}}\left[I\cos(\omega_0 t) - Q\sin(\omega_0 t)\right] + \\ &- m_{\mathrm{op}}\,\mathrm{e}^{-\mathrm{j}\varphi_{\mathrm{op}}}\,\frac{1}{2}\left[\left(I^2 - Q^2\right)\cos(2\omega_0) - 2IQ\sin(2\omega_0)\right] \end{aligned} \tag{4}$$

where v_{ic}, and v_{oc}, correspond to the magnitudes of the input and output signals of the carrier amplifier transistor at the fundamental frequency, whereas v_{ip} and v_{op} signifies the magnitude of the input and output signal of the peaking amplifier transistor at the fundamental frequency.

The distorted DA output current (i_{out}) analyzed for the IM3 products is represented by (5) when approach-1 is used, and by (6) for the application of approach-2. Equations (7) and (8) encompass the IM5 products for linearization approaches, 1st and 2nd, respectively.

The 1st and 2nd terms in (5) and (6) represent the DA linearity deterioration produced by the 3rd order nonlinearity of the DA carrier and peaking stages. The other terms of the 2nd order in (5) and (6) are the mixing products between the fundamental signals and the linearization signals inserted at the input and the output of the carrier PA transistor or at the outputs of both carrier and peaking PA transistor in the DA. The 2nd order nonlinear terms produced due to linearization signal injection can diminish the initially created IM3 distortion by proper adjustment of the magnitude and phase of the linearization signals based on the analysis [5, 6, 8].

The 1st and 2nd terms in (7) and (8) define the DA output current generated by the 5th order nonlinearity of the amplifier stages. The other terms of the 3rd order are the mixing products between the fundamental signals and the linearization signals from the first or the second approach and they can reduce the original IM5 products if their magnitudes as well as phases are correlated properly, [5], [8].

In the case of the single stage amplifier, the theoretical background is relayed on the 1st approach explanation. More details relating to the generation of signal for the linearization, terms in given equations and their influence on the linearization process were explained in our previous work in [5], [8].

$$\begin{aligned} i_{\text{out}}\Big|_{\text{IM3}}^{\text{1st}} = &\left[\frac{3}{4}\left(v_{\text{ic}}\right)^3 g_{\text{m3}} + \frac{3}{4}\left(v_{\text{ip}}\right)^3 g_{\text{m3}} + \frac{1}{2} m_{\text{ic}}\,\mathrm{e}^{-\mathrm{j}\varphi_{\text{ic}}} v_{\text{ic}} g_{\text{m2}} + \right. \\ &\left. -\frac{1}{4} m_{\text{oc}}\,\mathrm{e}^{-\mathrm{j}\varphi_{\text{oc}}} v_{\text{ic}} g_{\text{m1d1}} + \frac{1}{4} m_{\text{ic}}\,\mathrm{e}^{-\mathrm{j}\varphi_{\text{ic}}} v_{\text{oc}} g_{\text{m1d1}}\right]\left(I^2+Q^2\right) \\ &\left(I\cos\left(\omega_0 t\right) - Q\sin\left(\omega_0 t\right)\right), \end{aligned} \tag{5}$$

$$\begin{aligned} i_{\text{out}}\Big|_{\text{IM3}}^{\text{2nd}} = &\left[\frac{3}{4}\left(v_{\text{ic}}\right)^3 g_{\text{m3}} + \frac{3}{4}\left(v_{\text{ip}}\right)^3 g_{\text{m3}} - \frac{1}{4} m_{\text{oc}}\,\mathrm{e}^{-\mathrm{j}\varphi_{\text{oc}}} v_{\text{ic}} g_{\text{m1d1}} + \right. \\ &\left. -\frac{1}{4} m_{\text{op}}\,\mathrm{e}^{-\mathrm{j}\varphi_{\text{op}}} v_{\text{ip}} g_{\text{m1d1}}\right]\left(I^2+Q^2\right)\left(I\cos\left(\omega_0 t\right) - Q\sin\left(\omega_0 t\right)\right), \end{aligned} \tag{6}$$

$$\begin{aligned} i_{\text{out}}\Big|_{\text{IM5}}^{\text{1st}} = &\left[\frac{5}{8}\left(v_{\text{ic}}\right)^5 g_{\text{m5}} + \frac{5}{8}\left(v_{\text{ip}}\right)^5 g_{\text{m5}} + \frac{3}{2}\left(m_{\text{ic}}\right)^2 \mathrm{e}^{-\mathrm{j}2\varphi_{\text{ic}}} v_{\text{ic}} g_{\text{m3}} + \right. \\ &+\frac{1}{2}\left(m_{\text{oc}}\right)^2 \mathrm{e}^{-\mathrm{j}2\varphi_{\text{oc}}} v_{\text{ic}} g_{\text{m1d2}} - m_{\text{ic}} m_{\text{oc}}\,\mathrm{e}^{-\mathrm{j}\left(\varphi_{\text{ic}}+\varphi_{\text{oc}}\right)} v_{\text{oc}} g_{\text{m1d2}} + \\ &\left. +\frac{1}{2}\left(m_{\text{ic}}\right)^2 \mathrm{e}^{-\mathrm{j}2\varphi_{\text{ic}}} v_{\text{oc}} g_{\text{m2d1}} - m_{\text{ic}} m_{\text{oc}}\,\mathrm{e}^{-\mathrm{j}\left(\varphi_{\text{ic}}+\varphi_{\text{oc}}\right)} v_{\text{ic}} g_{\text{m2d1}}\right] \\ &\left(I^2+Q^2\right)^2\left(I\cos\left(\omega_0 t\right) - Q\sin\left(\omega_0 t\right)\right), \end{aligned} \tag{7}$$

$$\begin{aligned} i_{\text{out}}\Big|_{\text{IM5}}^{\text{2nd}} = &\left[\frac{5}{8}\left(v_{\text{ic}}\right)^5 g_{\text{m5}} + \frac{5}{8}\left(v_{\text{op}}\right)^5 g_{\text{m5}} + \right. \\ &\left. +\frac{1}{2}\left(m_{\text{oc}}\right)^2 \mathrm{e}^{-\mathrm{j}2\varphi_{\text{oc}}} v_{\text{ic}} g_{\text{m1d2}} + \frac{1}{2}\left(m_{\text{op}}\right)^2 \mathrm{e}^{-\mathrm{j}2\varphi_{\text{op}}} v_{\text{ip}} g_{\text{m1d2}}\right] \\ &\left(I^2+Q^2\right)^2\left(I\cos\left(\omega_0 t\right) - Q\sin\left(\omega_0 t\right)\right). \end{aligned} \tag{8}$$

4. Linearization of a Single Stage Amplifier

The broadband single stage PA that operates from 2 GHz to 6 GHz frequency was designed according to the instructions given in [12]. Figure 1 illustrates the schematic of the amplifier with the applied linearization circuit, while Table 1 gives the values of the characteristic impedances and electrical lengths of the designed single stage PA elements, as well as the capacitance values. The schematic was drawn by using Keysight Advance Design System (ADS) software [13]. The applied linearization approach utilizes the 2nd order nonlinear signals adequately formed and processed in magnitude and phase angle in the base-band. Those signals modulate the fundamental carrier 2nd harmonic and are inserted at the input and output of the amplifier transistor. The broadband PA was designed by using CGH40010F transistor [14], and its characteristics obtained in simulation for carrier frequency 3.5 GHz at 1-dB compression point where the output power is 33 dBm are: Transducer power gain is 12.34 dB, power added efficiency PAE is 16.2%, DC power consumption is 12.2 W.

The broadband PA was tested in the ADS simulation for the 5G FBMC, UFMC, and FOFDM signals at carrier frequency 3.5 GHz, useful signal frequency bandwidth of 100 MHz and output power around 24 dBm that is approximately 9 dB below 1-dB compression point. The 5G signals (FBMC, UFMC, FOFDM) were formed by using Keysight SystemVue [15] and MATLAB software.

Elements	Characteristic impedance [Ω]	Electrical length [°]
TL1	13.92	7.504
TL2	4.274	6.758
TL3	62.85	36.91
TL4	58.29	34.41
TL5	18.49	16.23
TL6	57.18	145.9
TL7	51.39	131.4
	Capacitance [pF]	
C1	4.723	
C2	3.147	

Tab. 1. Characteristic impedances, electrical lengths and capacitances of single stage PA elements.

The results of output signal power before and after the linearization are compared in Tab. 2 for useful signal channels, for the adjacent channels at ±100 MHz offset from the carrier frequency over 2 MHz bandwidth. Also, power improvement at these offsets is given in Tab. 2. Figure 2 shows the output spectrum before and after the application of the proposed linearization approach-1 for the mentioned output power and frequency bandwidth of the useful signal.

It can be observed from Tab. 2 and also from the figures that the FOFDM signals have the highest spectrum power at ±100 MHz offsets (where the dominant nonlinear intermodulation products are of the 3rd order), then slightly lower power shows UFMC and the lowest intermodulation signal power is related to FBMC modulation format. The applied approach-1 achieves the best improvement at ±100 MHz offset over the 2 MHz band for the UFMC signals, then for the FBMC and slightly lower for the FOFDM, which can be seen in the exact number from Tab. 2.

5. Linearization of a Broadband Doherty Amplifier

The microstrip two-way Doherty amplifier for the broadband application in the frequency range of 0.9–1 GHz was designed by the ADS software in [16] in standard configuration with the quarter-wave impedance inverter and transformer in the output combining circuits with the characteristic impedance $R_0 = 50\ \Omega$ and $R_t = R_0/\sqrt{2}$, respectively, the 3dB quadrature branch-line coupler at the input to compensate for the phase difference of 90° caused by the 50 Ω quarter-wave impedance inverter at the output and two offset lines.

Based on the nonlinear MET model inserted into the ADS library for Freescale's MRF281S LDMOSFET [17], the broadband input (IMC) and output matching circuits (OMC)

Modulation	Output signal power [dBm]		Power at -100 MHz offset over 2 MHz band [dB]		Power at +100 MHz offset over 2 MHz band [dB]		Improvement at ±100 MHz offset over 2 MHz band [dB]	
	before	after	before	after	before	after	–	+
FBMC	23.83	23.93	–41.50	–58.25	–41.99	–56.65	16.75	14.66
UFMC	24.16	24.26	–39.96	–57.64	–40.94	–59.06	17.68	18.12
FOFDM	23.81	23.95	–34.99	–51.90	–37.02	–49.96	16.91	12.94

Tab. 2. Results of linearization for three 5G modulation formats at 24 dBm fundamental signals output power.

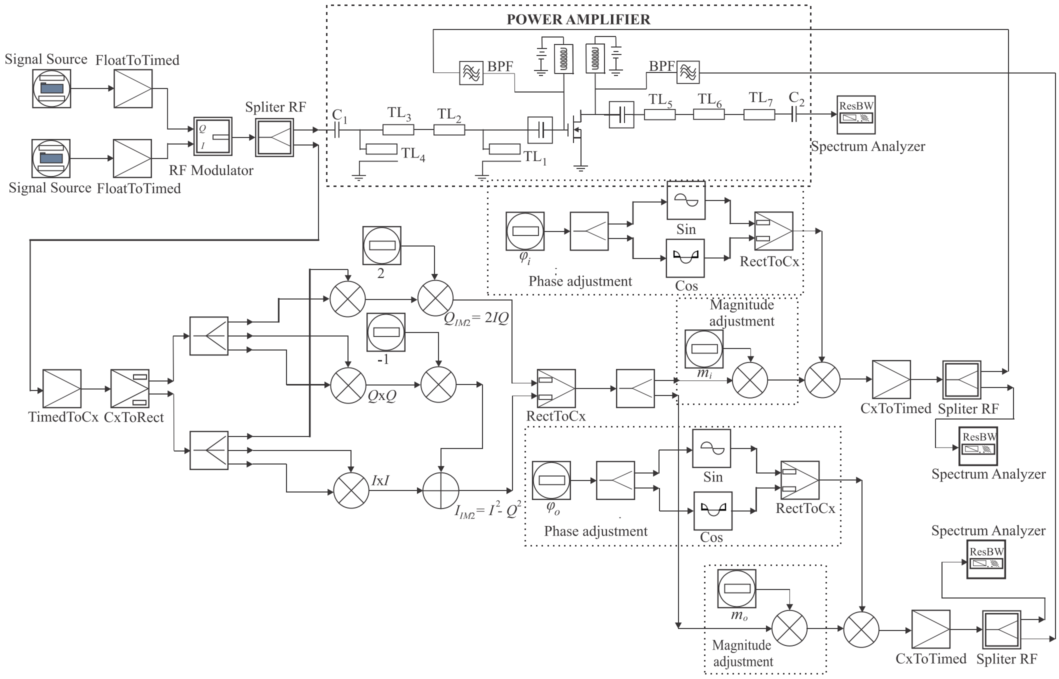

Fig. 1. ADS scheme of amplifier with the linearization circuit for 2nd harmonic injection modulated by digitally processed linearization signals.

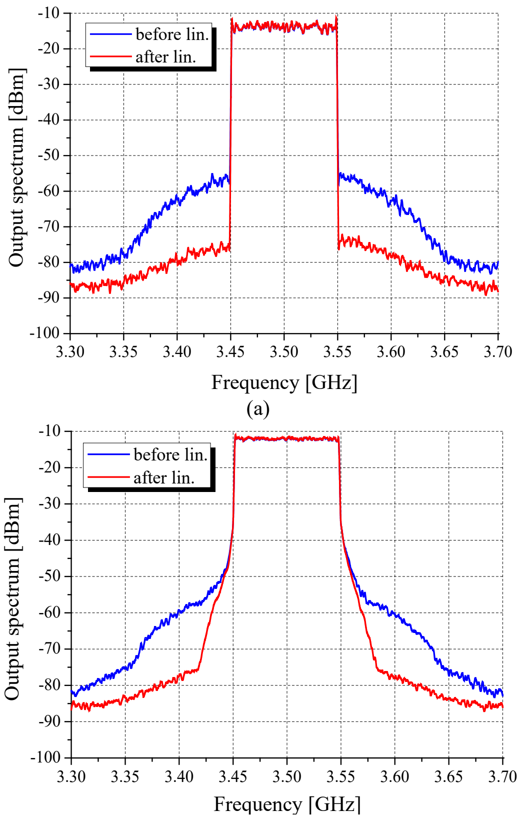

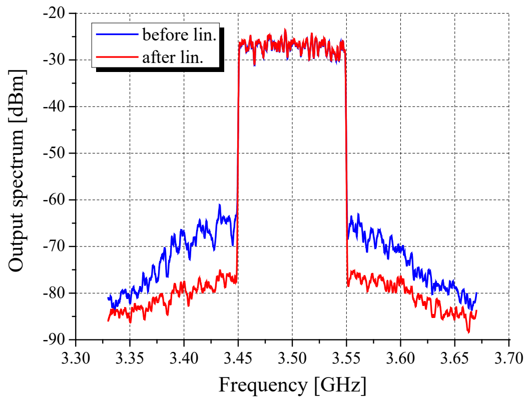

Fig. 2. Output spectrum before (blue line) and after (red line) linearization at 24 dBm output fundamental signal power and 100 MHz frequency bandwidth for modulation forms: a) FBMC, b) UFMC and c) FOFDM.

of the transistors in the carrier and peaking DA cells were designed using the filter structures. The design process of the broadband IMC and OMC of the amplifier includes a few steps starting from the configuration with the ideal lumped elements over the application of all necessary transformations until the realization of the microstrip circuit adequate for practical applications. The matching circuits were designed by using appropriate source and load impedances determined by the source-pull and load-pull analysis for the operation of the carrier amplifier in class-AB ($V_D = 26$ V, $V_{GC} = 5.1$ V) and the peaking amplifier in class-C ($V_D = 26$ V, $V_{GP} = 3.6$ V). The DA maximum gain at 0.95 GHz obtained in simulation for a single-tone excitation is around 21 dB, the drain efficiency is maximally 58% at 30 dBm and 36% at 15 dBm input power levels. The Doherty amplifier layout including the hairpin band-pass filters, which are part of the linearization circuit, is illustrated in Fig. 3. The signals for linearization are injected into the input and output of the transistor in the amplifier stages over the hairpin filters.

The Doherty amplifier designed in microstrip technology was analyzed in simulation to evaluate two linearization approaches for the 5G FBMC modulation scheme. The tests were realized at 0.95 GHz carrier frequency (central frequency of 5G downlink standardization range) with useful channel spectrum bandwidth of 20 MHz for a range of output power levels up to 1-dB compression point. Simulated results, Fig. 4, compare the lower and upper adjacent channel power-ACP at dominant third-order intermodulation products at ±20 MHz offset from the carrier over 2 MHz bandwidth for two applied linearization approaches. After the DA linearization, the ACP was improved by approximately 10 dB for output power level up to 31 dBm, whereas the linearization grade decreased to 5 dB for maximal considered output power of around 34 dBm. It should be noticed that the output power of the useful signal increases when the linearization approaches are applied, especially in the case of approach-2. The denoted points in the figures correspond to the input power level of the useful signal 8 dBm to 12 dBm with the 2 dBm step. The linearization results achieved by approach-2 are slightly worse than in approach-1 for the lower output power

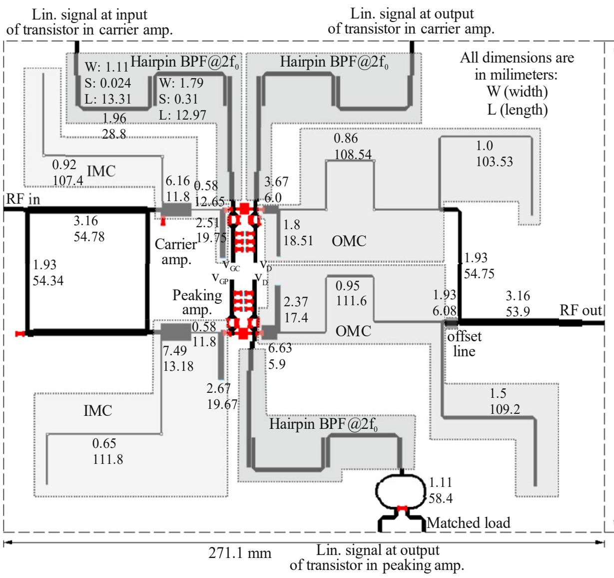

Fig. 3. Layout of broadband two-way microstrip DA including band-pass filters for the injection of the signals for linearization.

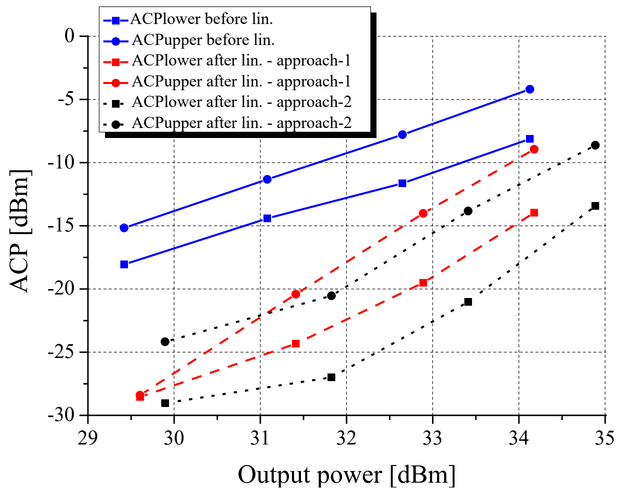

Fig. 4. ACPs of DA for 5G FBMC modulation with 20 MHz useful signal bandwidth in a range of power.

until 31 dBm and become better for approximately 2 dB for higher output power levels.

6. Measurement Set-Up

The setup depicted in Fig. 5 was established for the experimental validation of the linearization approaches developed by our research team. The measurement system was devised to facilitate the validation of these linearization approaches, which typically employ two linearization signals that, following digital processing in the baseband, modulate the second harmonic of the fundamental signal. This measuring system can generate three distinct and synchronized signals: the fundamental signal and two linearization signals at the frequency of the second harmonic of the fundamental signal.

The Analog Devices AD-FMCOMMS5-EBZ evaluation board, [18], was used as a signal generator unit. The AD-FMCOMMS5-EBZ is a high-speed analog module designed with two AD9361 chips enabling the construction of a 4×4 MIMO system, [19]. The AD9361 is a high-performance, highly integrated RF transceiver that operates within the frequency range of 70 MHz to 6 GHz and offers support for bandwidths ranging from less than 200 kHz to 56 MHz. Power is supplied to the board through two FMC connectors, allowing for seamless integration with the Zynq ZC706 FPGA platform, [20]. To manage communication and control of the FPGA platform featuring the FMCOMMS5 RF board, we leveraged the MATLAB environment in conjunction with the Communications Toolbox Support Package for Xilinx Zynq-Based Radio and Analog Devices Transceiver Toolbox Add-Ons. The fundamental signals and linearization signals originating from MATLAB were transmitted through the FPGA platform to the RF board. In this setup, one of the AD9361 transceivers had its central frequency set at the fundamental signal frequency using MATLAB, while the central frequency for

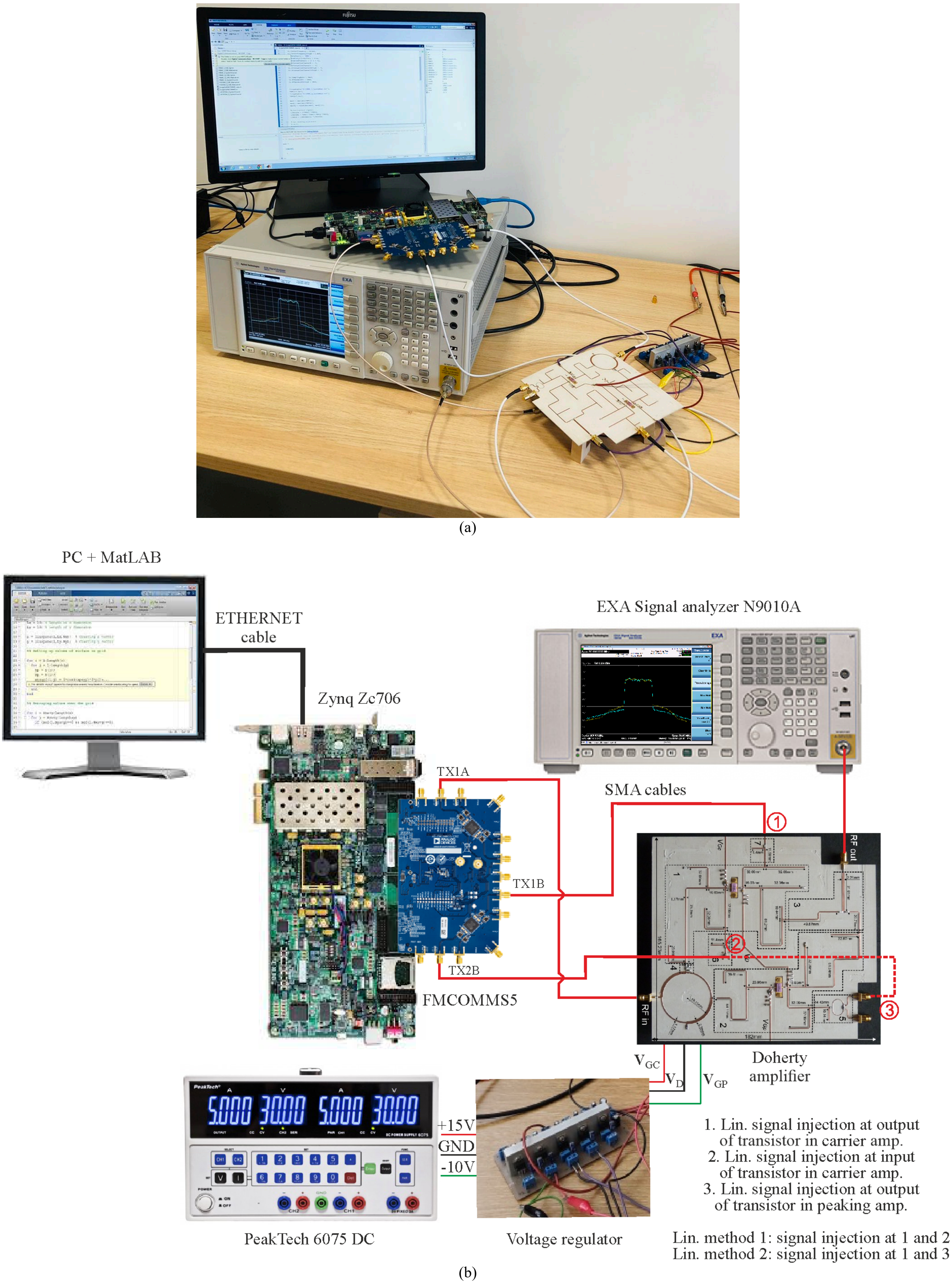

Fig. 5. Experimental verification of linearization approaches: (a) Lab photo; (b) schematic diagram.

the other AD9361 transceiver was set to the second harmonic of the fundamental signal. The first transceiver was employed for generating fundamental signals, while the second transceiver was dedicated to generating linearization signals at the frequency of the second harmonic of the fundamental signal.

To illustrate the outcomes of the linearization approaches, we utilized the Zynq ZC706 FPGA + AD-FMCOMMS5-EBZ platforms to generate the 5G FBMC signals, and to generate signals used for the linearization, which were controlled in the magnitude and phase in MATLAB. The impact of the linearization was assessed on a fabricated two-way asymmetric Doherty amplifier-ADA, operating at a central frequency of 0.9 GHz. We conducted measurements of the output spectra and adjacent channel power ratios (ACPRs) for both pre- and post-linearization states, considering the 5G FBMC modulation format and varying useful signal bandwidth. Measurement results were observed using the EXA Signal Analyzer N9010A.

The ADA achieves a maximum transducer gain of 9 dB during measurement [8]. This was attained by biasing the carrier amplifier in class-AB ($V_D = 5$ V, $V_{GC} = -3$ V), while the peaking amplifier operates in the class-C ($V_D = 5$ V, $V_{GP} = -5$ V) using the AP602A-2 GaAs MESFET transistor in the amplifying cells. The asymmetrical DA carrier and peaking PAs were designed with a Rogers 3010 substrate, which is 1.6 mm thick with a 17 µm metallization layer. Additionally, the measured 1-dB compression point of the amplifier occurs at an output power of 15 dBm, while ADA reaches a maximum output power of 18 dBm.

7. Experimental Results

The ADA was tested using the 5G FBMC signal at a 0.9 GHz carrier frequency with useful signal frequency bandwidths of 5 MHz, 7.5 MHz, and 10 MHz. The measurements were performed for the FBMC signal output power level 0 dBm for both described linearization approaches. It should be mentioned that the maximal power level is defined by the measured set-up equipment performances that is FMCOMMS5 RF board.

Figure 6 displays the output spectrum of the FBMC signal before and after the application of the two linearization approaches for the three considered frequency bandwidths. The figures demonstrate that the measurements provide highly comparable results for the FBMC signal for both applied linearization approaches for all inspected frequency bandwidths. The measured FBMC output spectrum for the in-band signal part retains the same shape for both implemented approaches, while out-of-band signal parts have resembling shapes but little diverse values. The results obtained from the measurements indicate that both approach-1 and approach-2 show similar results. However, the approach-2 resulted in a more symmetrical FBMC spectrum compared to approach-1.

Table 3 presents the ACPR improvement by linearization for the 5G FBMC signal of the considered frequency bandwidths observed at the corresponding offsets (±5 MHz, ±7.5 MHz, ±10 MHz) from the carrier frequency.

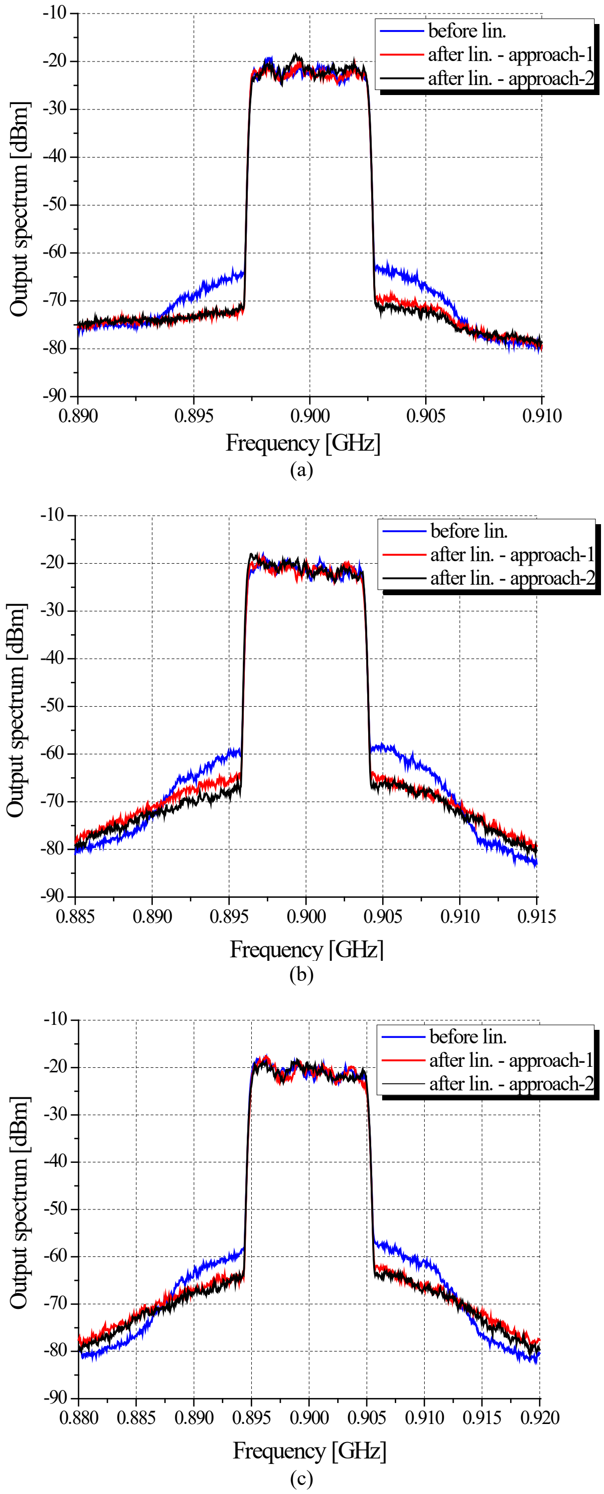

Fig. 6. Output spectrum for 5G FBMC signal for output signal power 0 dBm before (blue line) and after linearization by approach-1 (red line) and approach-2 (black line) for: (a) 5 MHz, (b) 7.5 MHz and (c) 10 MHz useful signal frequency bandwidth.

FBMC signal bandwidth [MHz]	Improvement [dB] approach-1		Improvement [dB] approach-2	
	–	+	–	+
5	at ±5 MHz offset			
	4.34	4.8	4.31	4.86
7.5	at ±7.5 MHz offset			
	3.12	5.18	5.3	5.17
10	at ±10 MHz offset			
	3.87	5.9	4.81	5.19

Tab. 3. Measured ACPR improvement for 5G FBMC modulation for three different useful signal frequency bandwidths.

8. Conclusion

Experimental linearization results acquired by two digital linearization approaches applied to the asymmetrical Doherty amplifier created in microstrip technology are presented in this paper, as well as simulation linearization results for the single stage power amplifier and the symmetrical microstrip Doherty amplifier. We analyzed the effect of the linearization approach that uses baseband signals of the 2nd order nonlinearity adequately shaped and processed in magnitude and phase in baseband and then modulates the 2nd harmonic of the fundamental useful signal carrier. The linearization signals formed in this way are then inserted at the input and output of the single stage PA transistor. The linearization was performed in simulation for the three most promising post-OFDM 5G modulation formats: FBMC, UFMC, and FOFDM when the useful signal bandwidth is 100 MHz. It can be inferred that a very satisfactory improvement in adjacent channels, where the 3rd order intermodulation products are dominant, was attained by applying the proposed linearization approach. It should be mentioned that the FOFDM modulation scheme has the worst linearity without linearization. Moreover, the UFMC signals were linearized by the most level but similar to the other 5G candidates. Moreover, a symmetrical Doherty amplifier designed in microstrip technology was tested in simulation for the 5G FBMC signal at 5G frequency range of around 0.95 GHz and 20 MHz useful signal bandwidth for the range of power. It can be spotted that the satisfactory results of linearization were achieved for two different approaches: when signals for linearization are inserted at the input and output of the transistor of the carrier amplifying stage (approach-1) and when they are run at the outputs of the two amplifier stages in the Doherty topology (approach-2) indicating that better linearization impact has latter linearization approach for the higher power up to 1-dB compression point. Furthermore, the fabricated asymmetrical microstrip Doherty amplifier was experimentally tested for the 5G FBMC signal at 5G frequency range of around 0.9 GHz and 5 MHz, 7.5 MHz, and 10 MHz useful signal bandwidths by the two mentioned linearization approaches. The measured results demonstrated that approach-1 and approach-2 give very similar linearization improvement for all analyzed signal bandwidths pointing that the linearization by approach-2 achieves a more symmetrical signal spectrum than by approach-1.

Acknowledgments

This work was supported by the Ministry of Education, Science and Technological Development of the Republic of Serbia (Grant No. 451-03-65/2024-03/200102) and Science Fund of the Republic of Serbia (Grant No. 6398983 - Serbian Science and Diaspora Collaboration Program: Vouchers for Knowledge Exchange – project name: Digital Even-Order Linearization of 5G Power Amplifiers in Bands below 6GHz - DELFIN).

References

[1] OSSEIRAN, A., MONSERRAT, J. F., MARSCH, P. (eds.) *5G Mobile and Wireless Communications Technology*. Cambridge University Press, 2016. DOI: 10.1017/CBO9781316417744

[2] ZAIDI, A., ATHLEY, F., MEDBO, J., et al. *5G Physical Layer: Principles, Models and Technology Components*. Elsevier Academic Press, 2018. ISBN: 978-0128145784

[3] BOREL, A., BARZDENAS, V., VASJANOV, A. Linearization as a solution for power amplifier imperfections: A review of methods. *Electronics*, 2021, vol. 10, p. 1–25. DOI: 10.3390/electronics10091073

[4] HAIDER, F. M., YOU, F., HE, S., et al. Predistortion-based linearization for 5G and beyond millimeter-wave transceiver systems: A comprehensive survey. *IEEE Communications Surveys & Tutorials*, 2022, vol. 24, no. 4, p. 2029–2072. DOI: 10.1109/COMST.2022.3199884

[5] ATANASKOVIĆ, A., MALEŠ-ILIĆ, N., BLAU, K., et al. RF PA linearization using modified baseband signal that modulates carrier second harmonic. *Microwave Review*, 2013, vol. 19, no. 2, p. 119 to 124. ISSN: 14505835

[6] ĐORIĆ, A., ATANASKOVIĆ, A., MALEŠ-ILIĆ, N., et al. Linearization of RF PA by even-order nonlinear baseband signal processed in digital domain. *International Journal of Electronics*, 2019, vol. 106, no. 12, p. 1904–1918. DOI: 10.1080/00207217.2019.1636145

[7] ATANASKOVIĆ, A., BUDIMIR, D., MALEŠ-ILIĆ, N., et al. Combination of digital second-order linearization technique and DPD compensation technique - concept and results. In *Proceedings of the 10th International Conference on Electrical, Electronic and Computing Engineering (IcETRAN 2023)*. East Sarajevo (Bosnia and Herzegovina), 2023, p. 1–5. DOI: 10.1109/IcETRAN59631.2023.10192197

[8] ATANASKOVIĆ, A., MALEŠ-ILIĆ, N., ĐORIĆ, A., et al. Doherty amplifier linearization by digital injection methods. *Facta Universitatis, Series: Electronics and Energetics*, December 2022, vol. 35, no. 4, p. 587–601. DOI: 10.2298/FUEE2204587A

[9] CAI, Y., QIN, Z., CUI, F., et al. Modulation and multiple access for 5G networks. *IEEE Communications Surveys & Tutorials*, 2018, vol. 20, no. 1, p. 629–646. DOI: 10.1109/COMST.2017.2766698

[10] BOZIC, M., BARJAMOVIC, D., CABARKAPA, M., et al. Waveform comparison and PA nonlinearity effects on CP-OFDM

and 5G FBMC wireless systems. *Microwave and Optical Technology Letters*, 2018, vol. 60, no. 8, p. 1952–1956. DOI: 10.1002/mop.31272

[11] PEDRO, J. C., PEREZ, J. Accurate simulation of GaAs MESFET's intermodulation distortion using a new drain-source current model. *IEEE Transactions on Microwave Theory and Techniques*, 1994, vol. 42, no. 1, p. 25–33. DOI: 10.1109/22.265524

[12] PENGELLY, R. *Large Signal Modeling of GaN HEMT Based Circuits.* January 2012, CREE.

[13] KEYSIGHT ADS, 2021. Santa Rosa (United States): Keysight Technologies, Inc.

[14] MACOM TECHNOLOGY SOLUTIONS INC. *CGH40010 10 W, DC - 6 GHz, RF Power GaN HEMT by Cree/Wolfspeed/MACOM for General Purpose Broadband Applications.* Datasheet, Rev 4.4. [Online] Cited 2022-10-28. Available at: https://cdn.macom.com/datasheets/CGH40010.pdf

[15] KEYSIGHT SYSTEMVUE, 2020. Santa Rosa (United States): Keysight Technologies, Inc.

[16] MALEŠ-ILIĆ, N., ĐORIĆ, A., ATANASKOVIĆ, A. Linearization of broadband two-way microstrip Doherty amplifier. *Facta Universitatis, Series: Electronics and Energetics*, 2016, vol. 29, no. 1, p. 127–138. DOI: 10.2298/FUEE1601127M

[17] FREESCALE SEMICONDUCTOR/NXP. *MRF281S, 2000 MHz, 4 W, 26 V Lateral N-channel Broadband RF Power MOSFET.* Technical data, rev. 6, October 2008. [Online] Available at: https://www.nxp.com/docs/en/data-sheet/MRF281.pdf

[18] ANALOG DEVICES. *AD-FMCOMMS5-EBZ, Dual AD9361 Evaluation Board AD-FMCOMMS5-EBZ User Guide*. [Online]. January 2016. Available at: http: //wiki.analog.com/resources/eval/user-guides/ad-fmcomms5-ebz

[19] ANALOG DEVICES. *AD9361, RF 2×2 Agile Transceiver.* Data sheet, rev G. [Online]. June 2013. Available at: https://www.analog.com/media/en/technical-documentation/data-sheets/ad9361.pdf

[20] *Zynq ZC706 FPGA, AMD Zynq 7000 SoC ZC706 Evaluation Kit by AMD, UG954 - ZC706 Evaluation Board for the Zynq-7000 XC7Z045 SoC User Guide.* Version v1.8. [Online]. August 2019. Available: https://docs.xilinx.com/v/u/en-US/ug954-zc706-eval-board-xc7z045-ap-soc

About the Authors ...

Aleksandar ATANASKOVIC received the Dipl. Ing., M.Sc., and Ph.D. degrees in Electrical Engineering from the Faculty of Electronic Engineering, University of Nis, Serbia, in 1997, 2004, and 2015, respectively. His research interests include microwave active and passive circuits, microwave and RF power amplifiers, linearization techniques, and SDR/FPGA-based transceivers in wireless/microwave testing and prototyping.

Aleksandra DJORIC received her Dipl. Ing. and Ph.D. degrees in Electrical Engineering from the Faculty of Electronic Engineering, University of Nis, Serbia in 2010 and 2023, respectively. Her research interests include microwave circuits, microwave and RF power amplifiers, linearization techniques, wireless communication technologies. She is a member of the Organizing Committee of the International Conference on Advanced Technologies, Systems and Services in Telecommunications – TELSIKS; member of the Technical Program Committee of the International Scientific Conference on Information, Communication and Energy Systems and Technologies – ICEST.

Natasa MALES ILIC received the Dipl. Ing. and M.Sc. degrees in Electronic Engineering from the University of Nis, Nis, Serbia in 1992 and 1997, respectively, and the Ph.D. degree at the Department of Electronic Systems, University of Westminster, London, UK in 2004. She is presently a Full Professor at the Department of Telecommunications, Faculty of Electronic Engineering, Serbia. The professional orientation of Dr. Males-Ilic is toward microwave techniques and electronic, wireless communication technologies, and artificial neural network applications. Dr. Males-Ilic is the Editor in Chief of the national journal Microwave Review. She is an IEEE member, as well as a member of the IEEE Women in Engineering, the IEEE MTT-S Chapter of Serbia and Montenegro, and DAAD Alumni.

Biljana P. STOSIC received the B.Sc. (1999), M.Sc. (2004) and Ph.D. (2008) degrees in Electrical Engineering from the Faculty of Electronic Engineering, University of Nis, Serbia. Research interests: Methods for computer-aided modeling and analysis of planar microwave structures by wave digital approach; approximation theory for filter functions and digital signal processing. She is a Senior Member of IEEE, a chair of WiE Affinity Group (since 2011), and MTT-S Chapter (since 2023) of IEEE Serbia and Montenegro Section. She is a member of the Organizing Committee of the International Conference on Advanced Technologies, Systems and Services in Telecommunications (TELSIKS); of the Technical Program Committee of the International Scientific Conference on Information, Communication and Energy Systems and Technologies (ICEST) and the International Conference on Telecommunications and Signal Processing (TSP). In the period 2014–2022, she was the editor-in-chief of the journal Microwave Review.

Djuradj BUDIMIR received a Ph.D. in Electronic and Electrical Engineering from the University of Leeds, UK. In March l994, he joined the Department of Electronic and Electrical Engineering at Kings College London, University of London, UK. Since January 1997, he has been with the School of Computer Science and Engineering, University of Westminster, London, UK, where he is now a Reader of wireless communications and leads the Wireless Communications Research Group. He is also a Visiting Professor with the School of Electrical Engineering, University of Belgrade. He has published more than 350 papers in refereed journals and conference proceedings, five books/book chapters and software's. His expertise includes design of circuits from RF through μWave/mmWave to Terahertz frequencies for 4G, 5G, B5G and 6G wireless communications, WLAN, WPT, wireless sensors, and Internet of Things (IoT).